*CORRESPONDENCE
Graciela Tejada
✉ gracielatejadap@gmail.com

CO$_2$ emissions in the Amazon: are bottom-up estimates from land use and cover datasets consistent with top-down estimates based on atmospheric measurements?

Graciela Tejada[1]*, Luciana V. Gatti[1,2], Luana S. Basso[1],
Henrique L. G. Cassol[1], Celso H. L. Silva-Junior[3,4,5],
Guilherme Mataveli[1], Luciano Marani[1], Egidio Arai[1],
Manuel Gloor[6], John B. Miller[7], Camilla L. Cunha[1],
Lucas G. Domingues[1,2], Alber Ipia[1], Caio S. C. Correia[1,2],
Stephane P. Crispim[1], Raiane A. L. Neves[1] and Celso Von Randow[1]

[1]General Coordination of Earth Science (CGCT), National Institute for Space Research (INPE), São José
dos Campos, Brazil, [2]Nuclear and Energy Research Institute (IPEN), São Paulo, Brazil, [3]Amazon
Environmental Research Institute, Brasília, Brazil, [4]Graduate Program in Biodiversity Conservation,
Federal University of Maranhão, São Luís, Brazil, [5]Department of Geography, School of Environment
Education and Development (SEED), The University of Manchester, Manchester, United Kingdom,
[6]School of Geography, University of Leeds, Leeds, United Kingdom, [7]Global Monitoring Laboratory,
National Oceanic and Atmospheric Administration (NOAA), Boulder, CO, United States

Amazon forests are the largest forests in the tropics and play a fundamental role
for regional and global ecosystem service provision. However, they are under
threat primarily from deforestation. Amazonia's carbon balance trend reflects
the condition of its forests. There are different approaches to estimate large-
scale carbon balances, including top-down (e.g., CO$_2$ atmospheric measurements
combined with atmospheric transport information) and bottom-up (e.g., land use
and cover change (LUCC) data based on remote sensing methods). It is important
to understand their similarities and differences. Here we provide bottom-up
LUCC estimates and determine to what extent they are consistent with recent
top-down flux estimates during 2010 to 2018 for the Brazilian Amazon. We
combine LUCC datasets resulting in annual LUCC maps from 2010 to 2018
with emissions and removals for each LUCC, and compare the resulting CO$_2$
estimates with top-down estimates based on atmospheric measurements. We
take into account forest carbon stock maps for estimating loss processes, and
carbon uptake of regenerating and mature forests. In the bottom-up approach
total CO$_2$ emissions (2010 to 2018), deforestation and degradation are the largest
contributing processes accounting for 58% (4.3 PgCO$_2$) and 37% (2.7 PgCO$_2$)
respectively. Looking at the total carbon uptake, primary forests play a dominant
role accounting for 79% (−5.9 PgCO$_2$) and secondary forest growth for 17% (−1.2
PgCO$_2$). Overall, according to our bottom-up estimates the Brazilian Amazon is a
carbon sink until 2014 and a source from 2015 to 2018. In contrast according to
the top-down approach the Brazilian Amazon is a source during the entire period.
Both approaches estimate largest emissions in 2016. During the period where flux
signs are the same (2015–2018) top-down estimates are approximately 3 times
larger in 2015–2016 than bottom-up estimates while in 2017–2018 there is closer
agreement. There is some agreement between the approaches—notably that the
Brazilian Amazon has been a source during 2015–2018 however there are also
disagreements. Generally, emissions estimated by the bottom-up approach tend

to be lower. Understanding the differences will help improve both approaches and our understanding of the Amazon carbon cycle under human pressure and climate change.

1. Introduction

Amazon forests are the greatest continuous tropical forest in the world, fundamental for the maintenance of global ecosystem services including carbon sequestration, water supply, climate regulation, and hosting an incredible amount of biodiversity. In the carbon budget over past decades, primary Amazon forests have been attributed to be the main tropical carbon sink (Pan et al., 2011). Because of the large extent of Amazonia, anthropogenic or climate perturbation can have impacts on the global carbon cycle (Aragão et al., 2014). Brazil has 49% of the Amazon forests but is also the country with the highest net deforestation reaching 18% of the Brazilian Amazon biome in 2021 (INPE, 2022). Between 2004 and 2012, deforestation decreased by 80% reaching its lowest level in 2012 with 4,571 km^2. From there, deforestation has been increasing again, reaching 13,038 km^2 in 2021 (INPE, 2022). Decades of deforestation, degradation, and fragmentation have increased the vulnerability of a large portion of these forests to global change impacts including droughts and anthropogenic fires as well (Aragão et al., 2014; Silva et al., 2020).

Trends in the carbon balance are a large-scale indicator of how these forests are responding to external pressures. There are different approaches to estimating carbon balances, which can broadly be classified as "top-down" and "bottom-up." Bottom-up approaches use local information, which is then upscaled spatially. Such information may range from plot scale forest inventory data to eddy fluxes towers results (local scale) to regional scale remote sensing-based land use and cover maps. Top-down approaches exploit the information about sources and sinks contained in spatial and temporal patterns of atmospheric CO_2 (and CO) dry air molar fractions. To extract this information, atmospheric transport models are used in an inverse mode (so-called atmospheric transport inversions; Cassol et al., 2020). Previous studies comparing both approaches show that the bottom-up approaches provide detail that the top-down atmospheric approach does not capture; in addition, when upscaling local data to the entire Amazon, differences begin to appear. That is why it is necessary to understand CO_2 fluxes from deforestation, forest degradation, and secondary forest separately (Grace, 2016).

As in many tropical countries, more than 46% of Brazilian greenhouse gas (GHG) emissions come from land use and cover change (LUCC; Albuquerque et al., 2020; MCTI, 2020a). LUCC and biomass content in forests are the base for the carbon emissions and removal estimations in tropical countries (Aguiar et al., 2012; Baccini et al., 2012; Harris et al., 2012). There are several regional LUCC datasets (maps) for the Brazilian Amazon, derived from Landsat images. Between them is the Project for Remote

Deforestation Monitoring (PRODES) project, which measures the annual and official deforestation rate in the Brazilian Legal Amazon since 1988. TerraClass is a project that maps the land use and cover of PRODES deforested areas, but only for the years 2004, 2008, 2010, 2012, and 2014 (Almeida et al., 2016). Also, the Brazilian Institute of Geography and Statistics (IBGE) has LUCC datasets for the years 2010, 2012, 2014, 2016, and 2018 (IBGE, 2016, 2018). MapBiomas is a collaborative network (Souza et al., 2020), which provides annual LUCC datasets also derived from Landsat images, from 1985 to 2021. However, none of these datasets cover all the LUCC processes related to forest degradation, secondary forest spatial coverage, and deforestation or the same temporal scale (e.g., annual LUCC).

Estimates from the top-down lower troposphere greenhouse gas (GHG) monitoring program (CARBAM; Gatti et al., 2014, 2021) covering 9 years (2010–2018) based on *in situ* flight atmospheric CO_2 measurements at four sites of the Brazilian Amazon indicate a decreasing capacity of the Amazon forests to absorb carbon as a result of deforestation and climate change patterns in the most deforested part of the Amazon (southeast). Gatti et al. (2021) found a correlation between the total PRODES deforested areas, the decrease in forest CO_2 removals, and high fire emissions from 2010 to 2018. To better understand these top-down flux results, it is important to compare them with bottom-up LUCC dynamics data for the same areas.

The purpose of this study is to provide bottom-up LUCC estimates and to determine whether they help understand and are consistent with the CARBAM top-down CO_2 atmospheric fluxes estimates from 2010 to 2018. Here, we assess LUCC (including secondary forest and forest degradation) CO_2 flux estimates in four regions of the Amazon and compare them with the CO_2 flux estimates based on atmospheric CO_2 and CO vertical profiles and the trajectory-based atmospheric transport inverse model (Gatti et al., 2021).

For this purpose, we merged different LUCC datasets. For land use and land cover and forest loss, we used MapBiomas collection 4.1 (MapBiomas, 2020); for degradation, we used the data from Bullock et al. (2020), and for secondary forest gain and loss, we used the data from Silva et al. (2020). Using an annual LUCC map from 2010 to 2018, we calculated the emissions and removals with a methodology specific to each LUCC class, also considering forest biomass. Then, we compared both approaches (top-down and bottom-up), remarking on their similarities and differences. We also state the limitations of the top-down, LUCC, and biomass data when understanding the bottom-up flight atmospheric measurements approach.

2. Materials and methods

We generated LUCC bottom-up CO_2 estimates and compared them with the results of the top-down study of Gatti et al. (2014, 2021). We first explain the process of estimating the top-down fluxes based on atmospheric CO_2 concentration of dry air molar fraction vertical profiles. We also discuss the determination of representative regions of top-down flux estimates, referred to as "influence regions." Then, we describe how we merged the different LUCC datasets to have an annual map from 2010 to 2018 for each influence region. Finally, we explain the specific analyses to calculate the emission/removal factors by LUCC class in the bottom-up approach.

2.1. Top-down atmospheric measurements and regions of influence (study area)

There are four sites in the Brazilian Amazon where the top-down flight atmospheric measurements were collected (Gatti et al., 2014, 2021). The sites are ALF (8.8°S, 56.7°W) at the southeast, SAN (2.8°S, 54.9°W) at the northeast, RBA (9.3°S, 67.6°W) at southwest-central, and TAB (5.9°S, 70.0°W) until 2012, which has been replaced by TEF in 2013 (3.7°S, 66.5°W), at northwest central region (Figure 1). The influence region of each flight site is estimated as the envelope of backward air mass trajectories reaching the sites. In this study, we have considered the mean annual influence region of all years (2010–2018) of each flight collection site (Figures 1B–F) to estimate the bottom-up emissions and removals. Our study area follows the Brazilian Amazon forest biome delimitation of Olson et al. (2001) with an area of 4,215,763 km² (Figure 1A; from now on, we will refer to it as the Brazilian Amazon) and the influence regions of TAB, TEF, RBA, SAN, and ALF inside the Brazilian Amazon (Figures 1B–F).

At the air-sampling sites, samples were collected in a descending vertical profile from 4,420 m above sea level (a.s.l.) to ~300 m a.s.l. The sampling system was installed on board in a small aircraft. All vertical profiles were made during the period when the planetary boundary layer tends to be well-mixed (between 12:00 and 13:00 local time), such that the profiles integrate gas fluxes from large regions under its region of influence. Air samples were analyzed by a non-dispersive infrared analyzer for CO_2 and by gas chromatography with HgO reduction detection for CO.

For each vertical profile, the flux from the influence region of the site was estimated as the difference of ΔCO_2 of the observed vertical profile CO_2 mole fraction at the site, a so-called background mole representing the amount of CO_2 of the atmospheric column entering the Amazon from the tropical Atlantic via the trade winds. Then, ΔCO_2 is divided by the travel time of air parcels from the Atlantic, to the vertical profiling site, obtaining an average CO_2 flux estimate for the influence region of the site, following the equation:

$$F_{CO2} = \int_{surface}^{4.4\ km} \frac{CO_{2,SITE}(z) - CO_{2,bg}}{t(z)} dz$$

where CO_2 is carbon dioxide dry air mole fraction in units of (mol m⁻³), z is the height above sea level (m), and $t(z)$ is air mass travel time (s) from the coast to the site at level z. A detailed description of the vertical profile sampling and flux calculation is available in Gatti et al. (2014, 2021) and Basso et al. (2016, 2021)'s studies.

The method to calculate the influence regions uses individual air parcel back trajectories of each vertical profile calculated by the Hybrid Single-Particle Lagrangian Integrated Trajectory Model (HYSPLIT; Stein et al., 2015). This model uses 1-h resolution to get the trajectory density (number of back trajectories passed over a 1 × 1° grid cell), between ~300 and 3,500 m a.s.l. A total of 590 CO_2 profiles (flights) from 2010 to 2018, considering a minimum density of trajectories of 2.5% were used. Detailed methods of the calculation of influence regions and weighted trajectory density are given by Cassol et al. (2020) and Gatti et al. (2021).

The top-down carbon flux estimate integrates the effect of all the surface sources and sinks between the coast and the sampling site, i.e., it is the total carbon flux due to all natural and anthropogenic surface sources and sinks including fire flux (biomass burning emission), fossil fuel emissions, and NBE flux (Net Biome Exchange: total flux minus the fire flux; Gatti et al., 2021).

2.2. LUCC annual map

We combine multiple Landsat-based datasets to represent annual LUCC related to forest carbon change (Table 1). Here, we describe the bottom-up datasets and methods to create the annual LUCC map from 2010 to 2018, including deforestation, secondary forest, and forest degradation processes. We calculated the LUCC areas for the Brazilian Amazon (Figure 1A) and the influence regions of each site (Figures 1B–F). For the forest class, we used the MapBiomas collection 4.1 dataset (MapBiomas, 2020), hereafter referred to MapBiomas.

As the secondary forest class is missing in MapBiomas, we obtained this class from Silva Junior et al. (2020), which is based on the same version of MapBiomas. A secondary forest is defined as a pixel with an anthropogenic class (e.g., agriculture or pasture) that turns into a forest again. The deforestation data were also derived from MapBiomas using an algorithm similar to that of Silva Junior et al. (2020). Deforestation is defined as a forest pixel that was replaced with any other class. For forest degradation, we used the data from Bullock et al. (2020), in which any pixel containing a forest disturbance is considered as forest degradation (e.g., selective logging, fire, and wind damage that did not result in a change in land cover or deforestation at a 0.09-ha scale). Bullock et al. (2020) methods used Landsat spectral endmember fractions to calculate the Normalized Degradation Fraction Index (NDFI). Other LUCC classes, planted forest, pasture, agriculture, and other non-forest natural formation, were obtained from MapBiomas as well. We merged some MapBiomas classes (Table 2) according to the Brazilian Third and Fourth National Communications on greenhouse gasses (3NC and 4NC; MCTI, 2016, 2020a) to the United Nations Framework Convention on Climate Change (UNFCCC) and the Brazilian System for Estimating Greenhouse Gas Emissions 8th (SEEG8) (Albuquerque et al., 2020; Alencar et al., 2020).
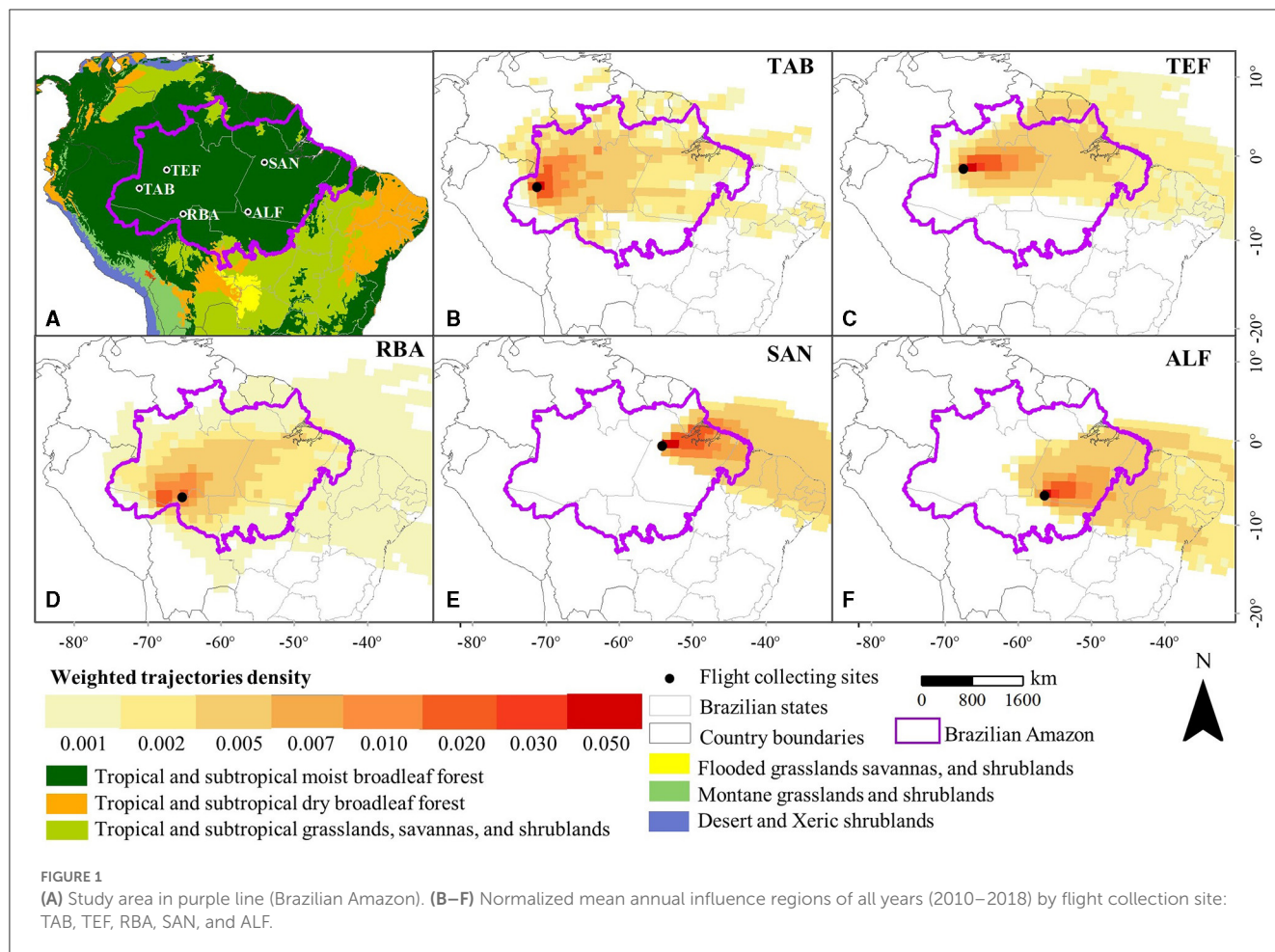
FIGURE 1
(A) Study area in purple line (Brazilian Amazon). **(B–F)** Normalized mean annual influence regions of all years (2010–2018) by flight collection site: TAB, TEF, RBA, SAN, and ALF.

TABLE 1 Land use and cover change datasets.

Process	LUCC dataset	Objective	Scale	Spatial resolution (m)	Temporal scale (years)	Sensor
Land use and cover	MapBiomas, 2020	Generate annual maps of land cover and use for Brazil	Brazil	30	Annual from 1988 to 2018	Landsat
Degradation	Bullock et al., 2020	Forest degradation	Brazil	30	1995 to 2018	Landsat
Secondary forest	Silva Junior et al., 2020	Secondary forest based on MapBiomas, 2020	Brazil	30	1986 to 2018	Landsat
Deforestation	MapBiomas, 2020	Map annual deforestation	Brazil	30	1988 to 2018	Landsat

Considering that the LUCC dataset employed different objectives and methods for mapping secondary forest (also secondary forest loss), degradation and deforestation classes, there may be some overlap between these classes. For example, one pixel classified as degradation by Bullock et al. (2020) can be classified as a secondary forest by Silva Junior et al. (2020). That is why we made an overlaying analysis between these datasets containing deforestation, degradation, and secondary forest gain and loss for 3 years (2010, 2014, and 2018). The overlaps between these classes are equal to or <1.8% of the total pixels (see Supplementary Table 1). Thus, we made our annual LUCC maps merging the datasets according to the order shown in Figure 2.

2.3. Bottom-up emission/removal factors

To quantify the CO_2 emissions and removals, different spatial analyses for each annual LUCC class in each influence region and within the Brazilian Amazon were made (Figure 3). In the case of TAB, we used the emission/removal estimates from 2010 to 2012 and for TEF from 2013 to 2018 because the TAB flight site was replaced by TEF in 2013. According to the IPCC (2006), to calculate GHG emissions, you multiply the activity data (our annual areas of each LUCC) by an emission/removal factor (representative value to quantify the emissions or removals). To designate emission/removal factors, we made a separate spatial
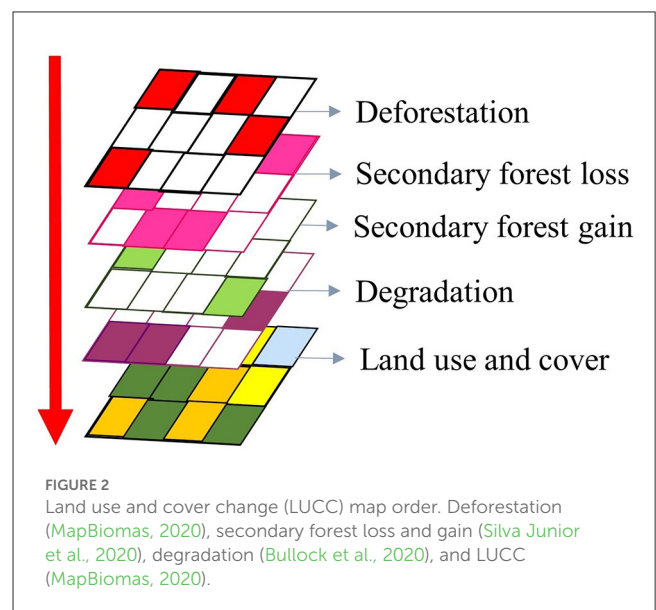
TABLE 2 Land use and cover change classes.

Selected classes	MapBiomas grouped subclasses (% of area)	% of each class area in 2010	LUCC spatial data source
1. Forest	Forest (79)	79.8	(MapBiomas, 2020) collection 4.1
	Mangrove (0.1)		
	Savanna (0.7)		
2. Secondary forest	Secondary forest*	2.5	Silva Junior et al., 2020
3. Degradation	Degradation*	0.3	Bullock et al., 2020
4. Secondary forest loss	Secondary forest loss*	0.2	Silva Junior et al., 2020
5. Deforestation	Deforestation*	0.2	Calculations based on Silva Junior et al. (2020) with data of MapBiomas (2020) collection 4.1
6. Planted forest	Forest plantation	0.01	(MapBiomas, 2020) collection 4.1
7. Other non-forest natural formation	Grassland (0.1)	3.3	(MapBiomas, 2020) collection 4.1
	Other non-forest natural formation (3.2)		
8. Pasture	Pasture (10.5)	10.5	(MapBiomas, 2020) collection 4.1
9. Agriculture	Annual and perennial crop (0.7)	0.7	(MapBiomas, 2020) collection 4.1
	Semi-perennial crop (0.001)		
10. Others	Urban infrastructure (0.1)	0.1	(MapBiomas, 2020) collection 4.1
	Other non-forest natural formation (0.004)		(MapBiomas, 2020) collection 4.1
	Beach and dune (0.0003)		
	Salt flat (0.005)		
	Mining (0.002)		
11. Water bodies	River, Lake, and Ocean (2.3)	2.3	(MapBiomas, 2020) collection 4.1
12. Non-observed	Not observed (0.2)	0.2	(MapBiomas, 2020) collection 4.1

*Classes not included in MapBiomas.

analysis for each LUCC (Figure 3). The detailed emission/removal factors ratios are described in Table 3.

The carbon stored in the forest and other non-forest natural formation classes also released into the atmosphere by deforestation, degradation, and secondary forest loss is determined by the biomass, assuming a carbon fraction of 0.5 in forest biomass (IPCC, 2006). To quantify the amount of carbon in the forest and the CO_2 emissions by deforestation and degradation, we used the carbon map of the 4NC (Fourth National Communications on greenhouse gasses) of Brazil to the UNFCCC (MCTI, 2020a). The 4NC map is based on field biomass (from the Brazilian Forest National Inventory and other projects) and airborne LiDAR data from the EBA project (EBA, 2016), which was extrapolated from 2016 to 2010 (the base of the 4NC; MCTI, 2020b). The 4NC carbon map represents the carbon stocks in 2010, including aboveground biomass, belowground biomass, dead wood, and litter, derived from carbon ratios of the aboveground biomass (MCTI, 2020b).

Intact forest carbon stocks are not accounted for in national communications (NCs) on greenhouse gases, which only consider
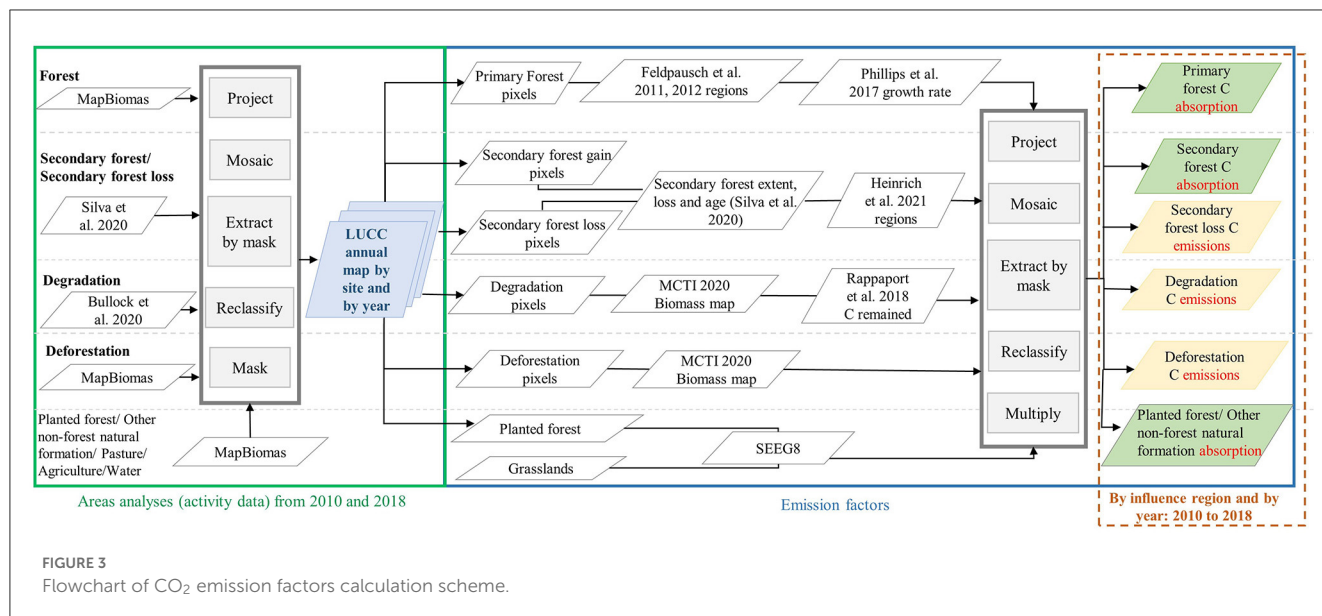

FIGURE 2
Land use and cover change (LUCC) map order. Deforestation (MapBiomas, 2020), secondary forest loss and gain (Silva Junior et al., 2020), degradation (Bullock et al., 2020), and LUCC (MapBiomas, 2020).

FIGURE 3
Flowchart of CO$_2$ emission factors calculation scheme.

TABLE 3 Emission factor ratios.

Classes	Emission/removals factors: ratios	Source
Forest	Biogeographic regions (shape file): Brazilian Shield (BrSh), southwest Amazon (SW), central-east Amazon (EC), the Guyana Shield (GuSh), and the central-west (W)	Additional file Supplementary Figure 1 of Feldpausch et al. (2011, 2012)
	Mean AGC (MgCha^{-1}yr^{-1}): BrSh −0.277; SW −0.444; EC −0.373; GuSH −0.412; W −0.482	Additional file Supplementary Table 1a of Phillips et al. (2017)
	Rations from AGC: palms, 4.6%; lianas, 3.1%; understory, 4.2%; deadwood, 8.8%; litter, 4.9%; belowground, 25.8%	Table 1, all data of Nogueira et al. (2008)
Secondary forest	Equation (1) of Heinrich et al. (2021): $Y_t = A\left(1 - e^{-kt}\right)^c \pm \varepsilon$; A, k and $c > 0$ Parameters for the equation of their Supplementary Table 9 "No disturbance" of each secondary forest growth region (shape file): southwest (SW), southeast (EC), northwest (NW), northeast (NE).	Equation (1), Supplementary Table 9, and secondary forest growth regions of Heinrich et al. (2021)
Degradation	Mean carbon	Carbon map of MCTI (2020a)
	Aboveground C loss 54,2%	Table 2 of Rappaport et al. (2018)
	Rations from AGC: deadwood loss, 46.9%; litter loss, 46.9%; belowground, 0%	Discussion point c of Withey et al. (2018)
Secondary forest loss	C loss in the year is the C content of the secondary forest of the previous year	Silva et al., 2020; Heinrich et al., 2021
Deforestation	Mean carbon	Carbon map of MCTI (2020a)
Planted forest	Mean carbon	Carbon map of MCTI (2020a)
Other non-forest natural formation	C stock: 0.52 MgCha^{-1}	SEEG8 Alencar et al. (2020)

C, Carbon; AGC, aboveground carbon.

anthropogenic emissions/removals. As carbon stock changes in intact forests are relevant for our study, we used the annual mean carbon change of ground forest biomass plots of RAINFOR (Phillips et al., 2017) from 2000 to 2009 (last decade with data). We used the forest class of the 4NC map only to account for the C stocks. The mean carbon change values for each Amazon biogeographic region [Brazilian Shield (BrSh), southwest Amazon (SW), the central-east Amazon (EC), the Guyana Shield (GuSh), and the central-west (W)] of Feldpausch et al. (2011, 2012) were multiplied by our total intact forest area of each biogeographic region (Table 3).

In the case of deforestation, we assumed that all the CO$_2$ from the forest carbon pools (aboveground biomass, belowground biomass, dead wood, and litter) is released to the atmosphere at the moment of the clear cut, the forest carbon data are from the 4NC map. To calculate the carbon removal and loss of secondary forest, we used the secondary forest extent and loss data of Silva Junior et al. (2020) and the secondary forest growth regions of Heinrich et al. (2021; Table 3). Furthermore, we assumed that the secondary forest carbon content of the prior year is released into the atmosphere the following year (secondary forest loss class).

For the forest degradation class, we used the 4NC biomass map as a base of forest biomass before degradation, assuming that 45.8% of aboveground carbon remains (54.2% of carbon is lost), according to Rappaport et al. (2018) and Assis et al. (2020). For belowground carbon, dead wood, and litter, see the ratios used in Table 3.

The removal factors (C stocks and annual increment) of other non-forest natural formation classes (which includes the grassland class) and planted forests class were obtained from the SEEG8 (based on the 3NC), which used the same MapBiomas LUCC classes. As we are focusing on the land use, land use change, and forestry (LULUCF) classes, in the carbon emissions or removal analyses, we excluded the classes: others, pasture, agriculture, water bodies, and non-observed. The SEEG8 and the 3NC (MCTI, 2016; Alencar et al., 2020) also do not include these classes. In the bottom-up approach, we are not including specifically the fire fluxes, even though part of fire fluxes is already included in the deforestation and forest degradation processes. Also, energy (fossil fuels), industrial processes, and agriculture sectors are not considered.

Each influence region has a different trajectory density; warmer colors represent the highest densities (Figures 1B–F). The bottom-up CO_2 emissions and removals were calculated using the weight of the trajectories' density. After calculating the CO_2 emissions and removals of the bottom-up approach, we compared them with the top-down CO_2 fluxes.

3. Results

3.1. Annual LUCC areas

To compare bottom-up with top-down estimates, we projected bottom-up analyses on the influence regions of each of the atmospheric CO_2 observation sites. The largest influence region is from RBA, covering 95% of the Brazilian Amazon area. TAB is the second largest area (82%), followed by TEF with 56%. RBA and TAB had the largest forest area in 2010 with 82 and 85%, respectively. TEF forest area was 82% of the total area in 2013. ALF (in the southeast) and SAN (in the northeast) have a smaller influence region with 35 and 16%, respectively, and the forest area in 2010 is also smaller (59 and 79% of the total area). All the annual LUCC areas are shown in Figure 4 and Supplementary Table 2, and their percentages in Figure 5. As observed in Figure 1, the influence regions may overlap and, therefore, are not cumulative.

In 2010, the Brazilian Amazon had 82% (3,265,968 km^2) of its area covered by forest. Between 2010 and 2018, ~97,066 km^2 of its forests were lost, an area larger than Portugal (Figure 4), even though it was only 3% of the Brazilian Amazon forested area. In the same period, the forest loss in the TEF region of influence was 43,239 km^2 (2%), in RBA 94,921 km^2 (3%), in SAN 29,036 km^2 (5%), and in ALF 50,031 km^2 (4%; Figure 5).

The second largest land use class in the Brazilian Amazon is pasture (452,039 km^2 in 2018; Figures 4, 5). It is also the class for which the total area varied the least. During the period 2010–2018, in the whole Brazilian Amazon, the pasture had increased by 10,455 km^2; in RBA, the pasture increased by 9,361 km^2 (Figure 5); in TAB, pasture remained constant; in TEF, the increase was 11,774

km^2 reaching 226,998 km^2 in 2018. In percentage, SAN (23%) and ALF (19%) have almost double the pasture area in 2018 than RBA (11%), TAB (9%), and TEF (11%). Agriculture was very small in TAB (1,123 km^2) and SAN (731 km^2) in 2010 and TEF (1,659 km^2) in 2013. In the Brazilian Amazon and RBA, agriculture areas almost doubled in 2018, reaching 1.4% (25,855 km^2). In ALF and SAN, the agricultural area tripled in 2018 compared with 2010, increasing 3,345 and 10,290 km^2, respectively. Secondary forest is the third largest LUCC class in all the influence regions. In ALF and SAN, the secondary forest percentage is larger than the other sites; these were 7.6% (48,879 km^2) in SAN and 4.7% (67,221 km^2) in ALF in 2010, reaching 9.3% (59,215 km^2) and 5.9% (84,242 km^2) in 2018, respectively (Figure 5).

The water class covers an area of 139,878 km^2, and the other non-forest natural formation class covers an area of 100,477 km^2. Other non-forest natural formation classes covered 2 and 3% by area in all influence regions except for TEF with 3.9% and SAN with 5.7%. Water class is also ~3%, except for SAN, which is the influence region with the most water at 5.2% (Supplementary Table 2).

The main LUCC classes related to carbon emissions including deforestation, degradation, and secondary forest loss cover a smaller area when compared to other LUCC classes, but they are by far the most important for carbon emissions. In general, secondary forest loss is larger than deforestation and degradation. Nonetheless, in dry years like 2010, 2015, and 2016, degradation emissions are larger than deforestation and secondary forest loss emissions. The area of these three classes increased at all sites, in terms of the percentage of each influence region, and is largest in ALF and SAN (Figure 5).

3.2. Forest carbon stocks

Forest carbon stocks are smaller near deforested areas. The mean forest carbon stocks for each influence region are shown in Figure 6 and Table 4. The highest carbon density areas are in the Guyana Shield biogeographic region, mainly northeast of TAB, TEF, and RBA, with a mean carbon stock of 316 MgCha^{-1}. The central-east Amazon biogeographic region has a mean carbon stock of 260 MgCha^{-1}, with high C stocks in the west and less in the east where part of ALF and SAN are, due to the high historical deforestation. The west biogeographic region covers the southwest of all influence regions, with lower carbon stocks than the central and north Amazon, with a mean of 202 MgCha^{-1}. The lowest carbon stocks are found in the southwest Amazon biogeographic region, with 172 MgCha^{-1} in part of Acre State, which also represents the smallest area.

The mean forest carbon stocks per influence region follow the same pattern, higher in the north, and northeast than in the central and eastern Amazon. TAB, TEF, and RBA have mean carbon stock close to 145 MgCha^{-1}. SAN has a small area of high carbon stocks in the northeast, but the rest are forest patches with less carbon density than the rest of the influence regions. ALF has more carbon stocks in the east, but in the southeast, there are forest patches with less carbon density. For both the SAN and ALF influence regions, the mean carbon stock is ~125 MgCha^{-1} (Table 4).
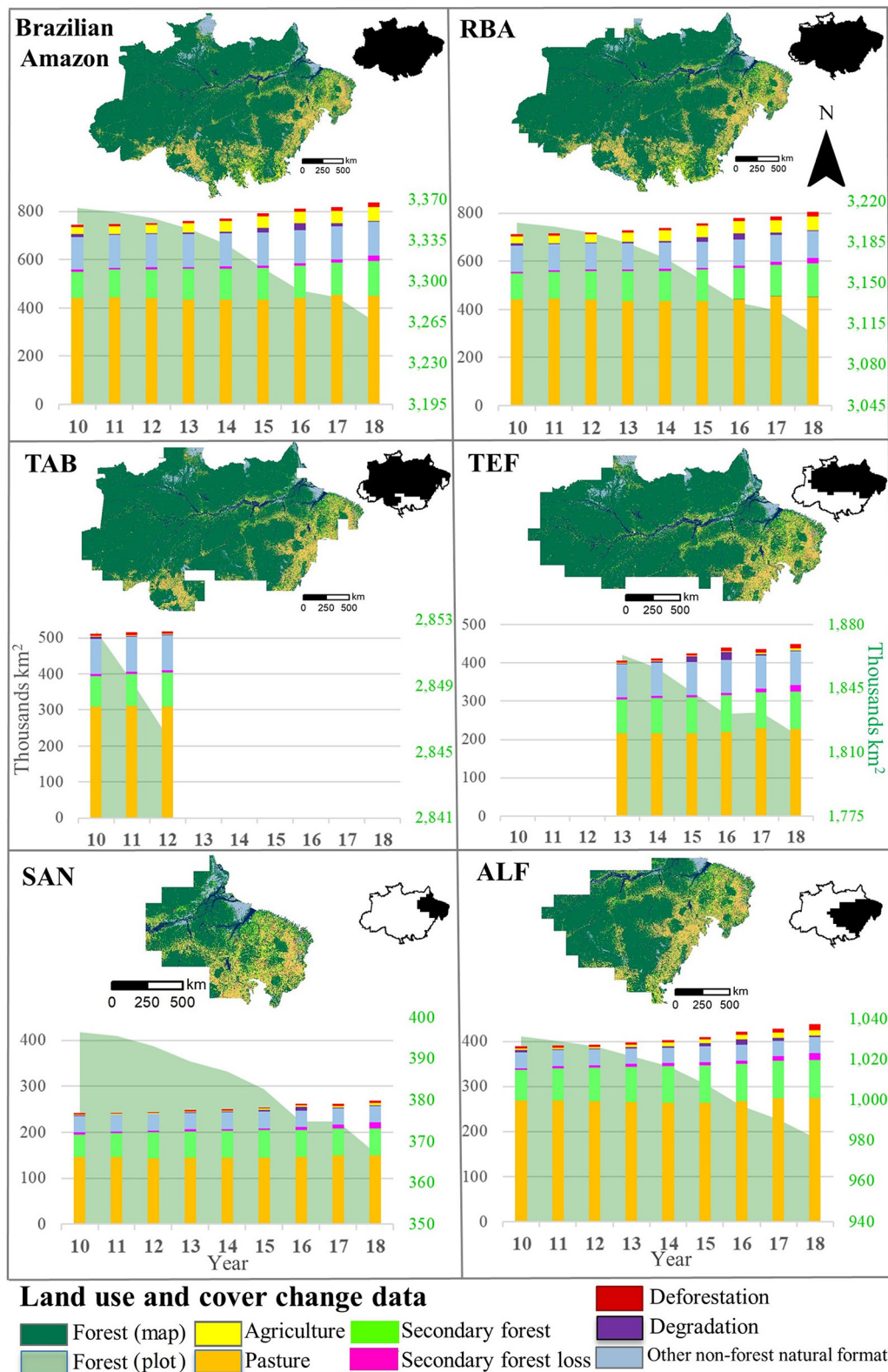
FIGURE 4
Land use and cover change (LUCC) in the Brazilian Amazon and each influence region. On the right Y axis are all the LUCC classes except forest which is represented in the left Y axis as area. Units are thousands of km^2. The legend applies to maps and bars; only the forest has a dark green for the map and a light green for the area graph. Detailed sources of the LUCC annual map are in Table 2. Detailed areas are in Supplementary Table 2.
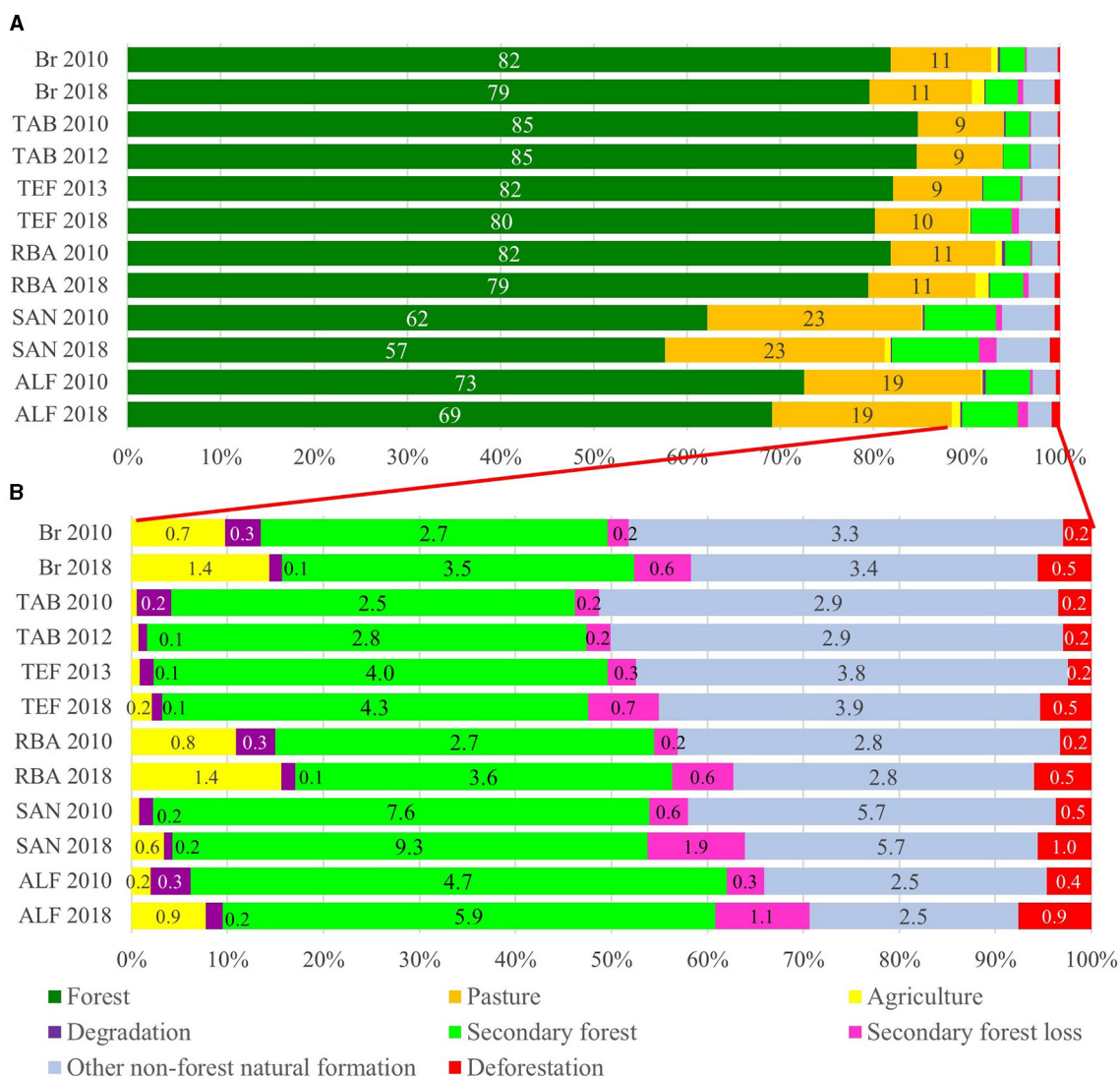
FIGURE 5
Percentage of land use and cover change (LUCC) in the Brazilian Amazon and each influence region in 2010 and 2018. **(A)** All LUCC classes; **(B)** LUCC without forest and pasture (to see better the rest of the classes).
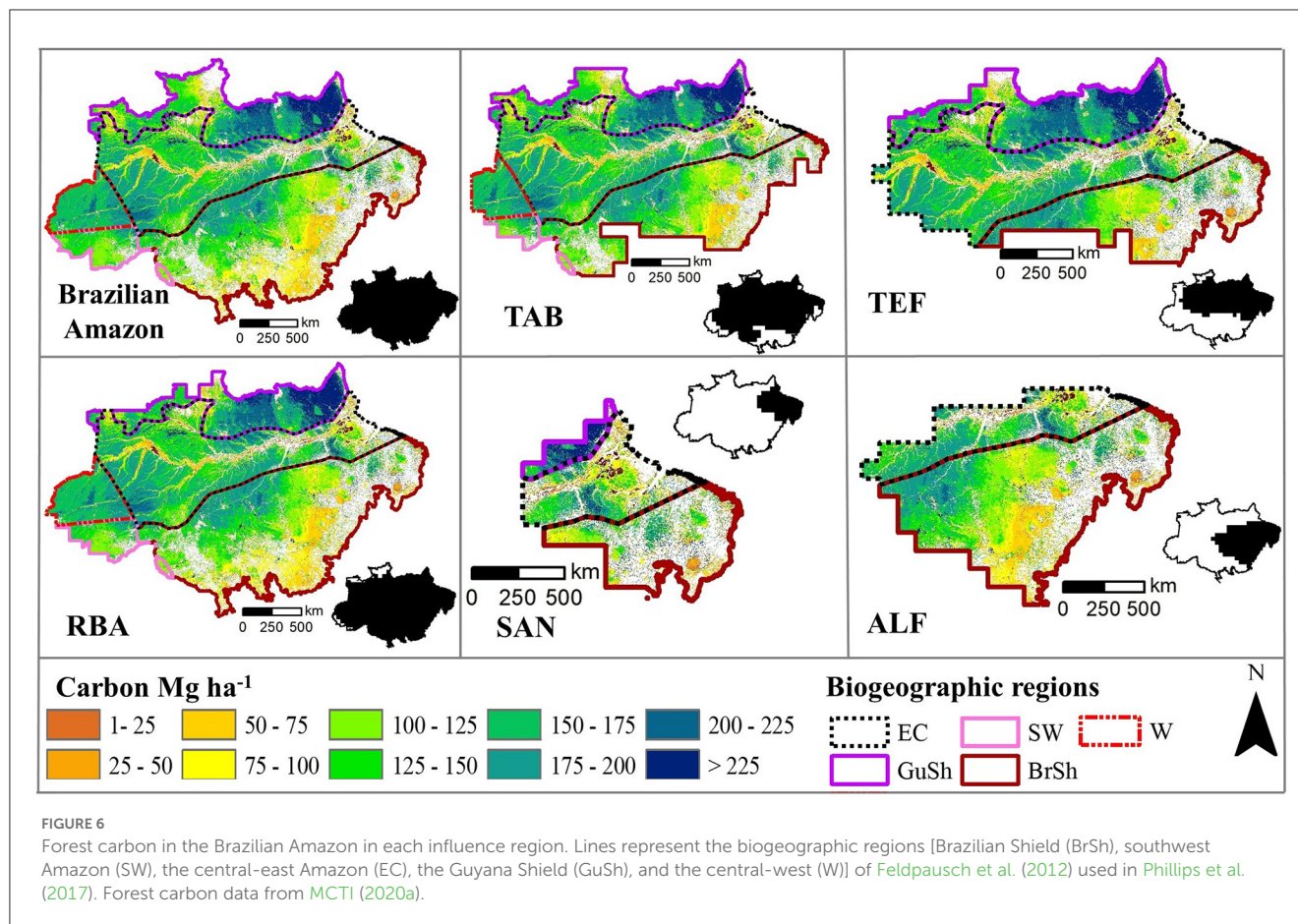
3.3. Top-down and bottom-up CO$_2$ emission and removal estimates

There are conspicuous differences between the bottom-up and top-down CO$_2$ fluxes in our study period (2010–2018), in both the Brazilian Amazon and each influence region (Figure 7 and Supplementary Table 3). First, we show the results of the bottom-up emissions and removal estimates considering the total (sum) fluxes from 2010 to 2018, also looking at each year and then the net bottom-up estimates (emissions less removals). In the case of top-down estimates, we show the total flux, fire flux, and NBE flux (total CO$_2$ estimates minus fire emissions; Figure 7). The top-down fire emissions are not explicitly considered in the bottom-up estimates, but deforestation, degradation, and secondary forest carbon loss emissions partially result from fire. Thus, we indicate the differences between the top-down total CO$_2$ flux with the net bottom-up CO$_2$ flux.

3.3.1. Bottom-up emissions

For the whole Brazilian Amazon, the bottom-up CO$_2$ emissions, deforestation, and degradation are the largest contributing classes with 58 and 37%, with a total emission (2010–2018) of 4,283 and 2,740 TgCO$_2$, respectively (Supplementary Table 3). Secondary forest loss emissions are smaller (6%) with a total emission of 417 TgCO$_2$.

When analyzing influence regions, total deforestation emissions (2010–2018) in RBA are 4,260 TgCO$_2$ and in TAB_TEF 2,018 TgCO$_2$, followed by degradation emissions with 2,598 and 2,004 TgCO$_2$, respectively. Secondary forest loss total emissions are smaller with 340 TgCO$_2$ in RBA and 200 TgCO$_2$ in TAB_TEF. Considering the relative proportion, for RBA and TAB_TEF deforestation is 59 and 48% and degradation is 36 and 47%, respectively, and secondary forest loss is 5% for both. For SAN and ALF, total deforestation CO$_2$ emissions represent 63 and 64%, degradation 31 and 30%, and secondary forest loss 6 and

FIGURE 6
Forest carbon in the Brazilian Amazon in each influence region. Lines represent the biogeographic regions [Brazilian Shield (BrSh), southwest Amazon (SW), the central-east Amazon (EC), the Guyana Shield (GuSh), and the central-west (W)] of Feldpausch et al. (2012) used in Phillips et al. (2017). Forest carbon data from MCTI (2020a).

8%, respectively. The total deforestation emissions for SAN and ALF are 1,412 and 2,371 $TgCO_2$, respectively, very large emissions considering that these influence regions have a smaller area than RBA and TAB_TEF (Figure 7 and Supplementary Table 3).

3.3.2. Bottom-up estimates of carbon uptake

Looking at the absorption process, primary forests play a fundamental role. From 2010 to 2018 primary forest absorption is 79% (−5,901 $TgCO_2$) in the Brazilian Amazon, 82% (−5,795 $TgCO_2$) in RBA, and 82% (−4,121 $TgCO_2$) in TAB_TEF. In SAN and ALF, primary forest absorption is 47% (−629 $TgCO_2$) in SAN and 67% (−1,554 $TgCO_2$) in ALF. Secondary forest growth is 17% (−1,243 $TgCO_2$) in the Brazilian Amazon, 14% (−1,018 $TgCO_2$) in RBA, 13% (−679 $TgCO_2$) in TAB_TEF, 43% (−582 $TgCO_2$) in SAN, and 27% (−625 $TgCO_2$) in ALF of total removal. The remaining fractional absorption is 3% for other non-forest natural formation classes in the Brazilian Amazon, RBA, TAB_TEF, and ALF, and 5% in SAN. Planted forest class accounts for 1% in the Brazilian Amazon and RBA and 2% in TAB_TEF, 3% in ALF, and 6% in SAN. More details can be found in Supplementary Table 3.

3.3.3. Net bottom-up estimates

In the bottom-up approach between 2010 and 2014, the net CO_2 flux (emissions less removals) is a sink in the Brazilian

Amazon and the TAB_TEF and RBA influence regions (Figure 7). Since 2015, these influence regions became a carbon source. In the case of SAN, during 2011 (−13 $TgCO_2yr^{-1}$) and 2012 (−17 $TgCO_2yr^{-1}$), the net flux was a sink; but in 2010, 2013, and 2014, the net flux was a source with <40 $TgCO_2yr^{-1}$, and from 2015 to 2018, it was a source with emissions between 81 and 338 $TgCO_2yr^{-1}$. For ALF, 2012 is the only year as a sink (−18 $TgCO_2yr^{-1}$), in 2011, 2013, and 2014 net flux was a source with <65 $TgCO_2yr^{-1}$, and from 2015 to 2018, net emissions ranged from 156 to 362 $TgCO_2yr^{-1}$ (Supplementary Table 3).

The year with the highest net carbon emissions from the bottom-up approach was 2016 in the Brazilian Amazon with 577 $TgCO_2yr^{-1}$, RBA with 471 $TgCO_2yr^{-1}$, and TAB_TEF with 450 $TgCO_2yr^{-1}$. SAN had 319 $TgCO_2yr^{-1}$ and ALF 292 $TgCO_2yr^{-1}$ in 2016, but the highest emission was in 2018 with 338 and 362 $TgCO_2yr^{-1}$, respectively. In all the influence regions, forest degradation area peaked in 2016 (Figure 4).

3.3.4. Top-down estimates

In the top-down approach, 2016 was also the year with the highest net emissions in the Brazilian Amazon (1,639 $TgCO_2yr^{-1}$) and the RBA (1,086 $TgCO_2yr^{-1}$) and ALF (950 $TgCO_2yr^{-1}$) influence regions. The exception is TAB_TEF with a peak in 2015 (540 $TgCO_2yr^{-1}$) and very low emissions in 2016 (23 $TgCO_2yr^{-1}$). For SAN, the highest emission year is 2012 (817 $TgCO_2yr^{-1}$) but

TABLE 4 Mean forest carbon stocks in the influence regions (ir), by biogeographic regions of Feldpausch et al. (2012) used in Phillips et al. (2017).

| | Amazon influence regions | | | Biogeographic regions | | | | | | | | | | | | | | |
| | | | | EC | | | GuSH | | | BrSh | | | W | | | SW | | |
	km²	%	Mean C MgCha⁻¹	km²	% of their ir	Mean C MgCha⁻¹	km²	% of their ir	Mean C MgCha⁻¹	km²	% of their ir	Mean C MgCha⁻¹	km²	% of their ir	Mean C MgCha⁻¹	km²	% of their ir	Mean C MgCha⁻¹
Brazil	4,215,763	100	141	1,332,867	31.6	307	703,228	16.7	316	1,724,585	40.9	297	248,981	5.9	202	201,240	4.8	172
TAB	3,465,180	100	147	1,119,642	32.3	304	598,535	17.3	308	863,006	24.9	293	180,518	5.2	203.33	77,020	2.2	168
TEF	2,362,080	100	148	914,064	26.4	297	503,540	14.5	308	437,915	12.6	260						
RBA	4,016,900	100	141	1,121,349	32.4	304	513,313	14.8	308	1,152,091	33.2	293	235,120	6.8	203	141,816	4.1	168
SAN	675,855	100	126	166,043	4.8	273	52,881	1.5	285	154,581	4.5	169						
ALF	1,470,310	100	124	298,732	8.6	250				713,810	20.6	289						

BrSh, Brazilian shield; SW, southwest Amazon; EC, central-east Amazon; GuSh, Guyana Shield; W, central-west.

high emissions also occurred in 2016 (651 $TgCO_2yr^{-1}$; Figure 7 and Supplementary Table 4).

3.3.5. Differences between top-down and bottom-up estimates

Comparing the total CO_2 top-down flux and the net bottom-up flux, we see that top-down estimates are considerably higher than the bottom-up estimates in the Brazilian Amazon. From 2010 to 2014, the bottom-up net flux is a sink, and in the total top-down approach, 2010–2018 is a source (Figure 7 and Supplementary Table 3). In 2010, the absolute difference between the approaches reaches 1,121 $TgCO_2yr^{-1}$, and in 2012, it is 1,588 $TgCO_2yr^{-1}$. Since 2015, both approaches are a source in the Brazilian Amazon, but 2015 and 2016 also exhibit a difference in the flux with 1,274 and 1,062 $TgCO_2yr^{-1}$, respectively. In 2017 and 2018, the differences are minor with 296 and 157 $TgCO_2yr^{-1}$, respectively.
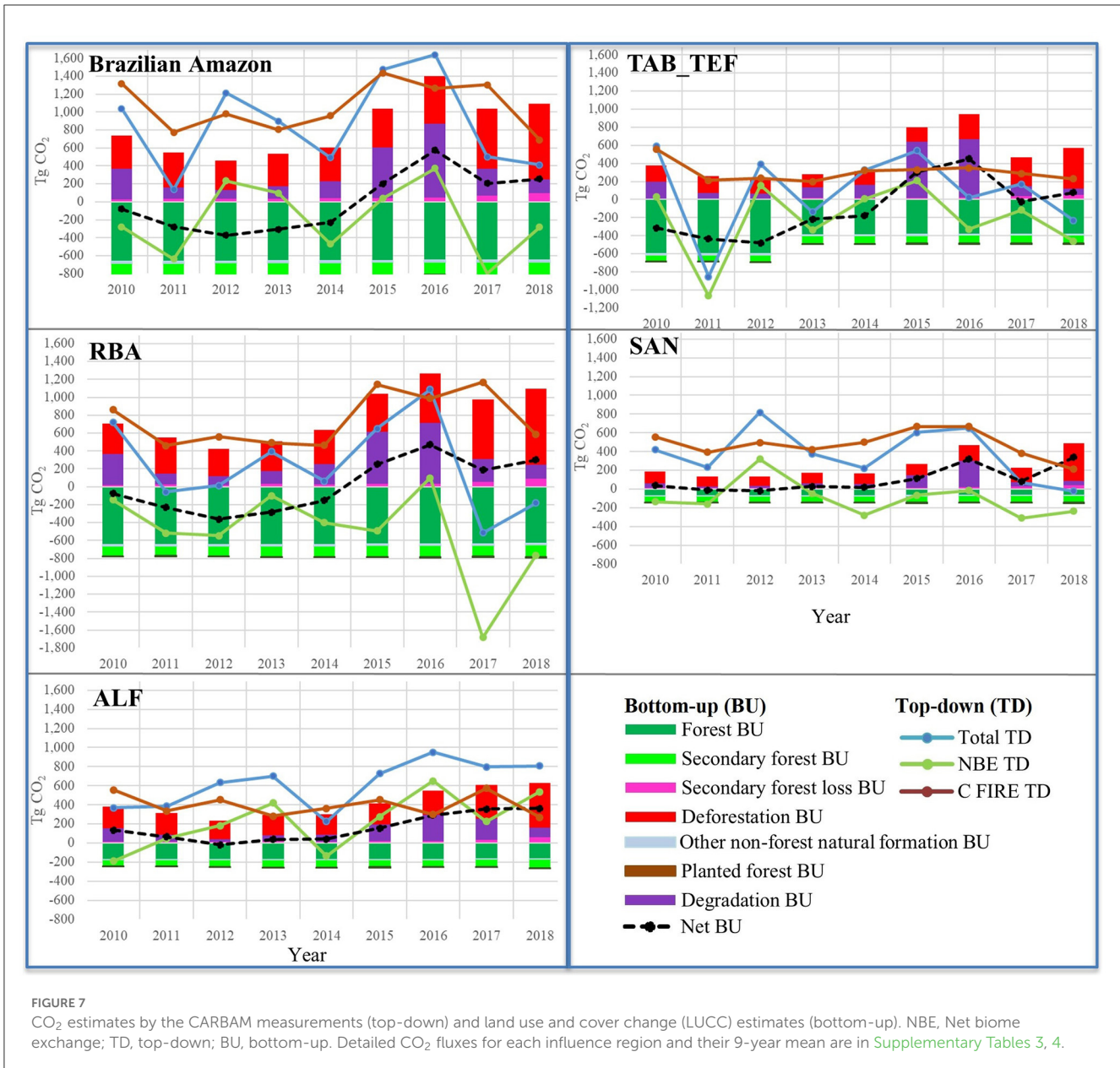
In the top-down total flux, TAB_TEF is a sink in 2011 (−854 $TgCO_2yr^{-1}$), 2013 (−138 $TgCO_2yr^{-1}$), and 2018 (−231 $TgCO_2yr^{-1}$). In 2018, the net bottom-up flux (76 $TgCO_2yr^{-1}$) in TAB_TEF is a source. In RBA, the total top-down flux is a sink in 2011 (−58 $TgCO_2yr^{-1}$), the same as the bottom-up flux (−229 $TgCO_2yr^{-1}$). In RBA, 2017 (−516 $TgCO_2yr^{-1}$) and 2018 (−180 $TgCO_2yr^{-1}$) top-down total fluxes are considerable sinks, opposite to the bottom-up fluxes, having an absolute difference of 704 and 482 $TgCO_2yr^{-1}$, respectively. For the rest of the years, the total top-down flux is a source in these influence regions with higher emissions in 2010 (589 $TgCO_2yr^{-1}$) and 2015 (540 $TgCO_2yr^{-1}$) for TAB_TEF and 2016 (1,086 $TgCO_2yr^{-1}$) for RBA. In ALF and SAN, the top-down fluxes suggest a net emission source in all years, also higher than the bottom-up estimates. The only exception is in SAN in 2018, the top-down total flux is a sink (−22 $TgCO_2yr^{-1}$), and the bottom-up net flux (338 $TgCO_2yr^{-1}$) is a source with an absolute difference of 361 $TgCO_2yr^{-1}$ (Figure 7).

4. Discussion

4.1. LUCC annual map

Constructing an annual LUCC map from 2010 to 2018 using several datasets was essential to show the relevance of the different LUCC dynamics, including deforestation, forest degradation, and secondary forest growth and loss. The forest is the largest class within the Brazilian Amazon, but anthropogenic activities related to pasture, secondary vegetation, deforestation, and forest degradation areas have a large extent. There are large and constant pasture areas that could be used to expand agriculture in the Brazilian Amazon and are also potential areas for secondary forest growth. Thus, some studies suggest that there is no need to open new deforestation frontiers (Souza et al., 2020).

The influence regions used in this study represent the annual mean air mass back-trajectory densities from all flights from 2010 to 2018, so we showed the annual LUCC in these areas. However, if additional years of atmospheric measurements (e.g., 2019 and 2020) are included, the number of trajectories would increase,

FIGURE 7
CO_2 estimates by the CARBAM measurements (top-down) and land use and cover change (LUCC) estimates (bottom-up). NBE, Net biome exchange; TD, top-down; BU, bottom-up. Detailed CO_2 fluxes for each influence region and their 9-year mean are in Supplementary Tables 3, 4.

and the boundary of each influence region may change. These modifications could impact the calculation of CO_2 fluxes.

Forest degradation, unlike deforestation, has challenges in terms of mapping and monitoring using remote sensing techniques (Costa et al., 2019). As a result, only a few datasets are available for this variable. Consequently, forest degradation is not currently included in NCs or SEEG GHG estimates (Wiltshire et al., 2022). However, our study along with the findings of Assis et al. (2020) indicates that forest degradation areas exceed deforestation and secondary forest loss during dry years (2010, 2015, and 2016). Therefore, we agree with the recommendation of Silva Junior et al. (2021), for the inclusion of forest degradation emissions in NCs.

As expected, the utilization of LUCC datasets employing different methodologies and approaches leads to variations in LUCC extent, consequently resulting in differences in CO_2 bottom-up estimates. Fortunately, LUCC datasets continue to progress. For

example, the new MapBiomas collections now include secondary forests, deforestation, and fire. Additionally, TerraClass and IBGE are preparing updated versions including new years. As a result, the accuracy and representation of LUCC will continue to improve.

4.2. Forest carbon stocks

The northeast Amazon region exhibits areas of high forest carbon stocks. Interestingly, these high-carbon areas also show significant divergences in biomass datasets, including both field measurements and biomass maps (Ometto et al., 2014; Tejada et al., 2020). On the other hand, areas with higher agreement between datasets, such as the southeast Amazon (Brazilian arc of deforestation), are located in regions with lower carbon stocks, closer to previously deforested or degraded forest areas.

The spatial and temporal scales of biomass maps present limitations for estimating CO_2 emissions/removals related to deforestation, degradation, and secondary forest dynamics. Biomass maps represent carbon stocks for specific years; for instance, the 4NC map represents the carbon stocks in 2010 and the Baccini et al. (2012) map represents the carbon stocks in 2000. Unfortunately, the availability of multitemporal (yearly) biomass data is insufficient to assess the carbon changes in secondary forests and degradation. However, with the advent of BIOMASS (Carreiras et al., 2017) and GEDi (Dubayah et al., 2022) new remote sensing missions, designed to have high-resolution, and improved temporal and spatial data, assessing secondary forest and forest degradation annual carbon change will become more feasible.

4.3. Bottom-up and top-down implications

For the bottom-up estimates, we aggregated several methodologies and approaches to designate the appropriate emission/removals factors for each LUCC class dynamics. Environmental factors influencing the growth of primary and secondary forests have been considered for carbon removal estimations. While primary forest carbon stocks are not considered in NCs (or SEEG), except for protected areas, they play a significant role in carbon sequestration. Therefore, we used the mean carbon change (growth of primary forest) derived from the RAINFOR field data (Phillips et al., 2017), considering the biogeographic regions determined by Feldpausch et al. (2011, 2012). The mean carbon change forest growth, as indicated by Phillips et al. (2017), shows a decline in carbon sink over the decades. We used the last decade of the study (2000–2010), which exhibits a 40% decrease in mean forest carbon change compared with the 1980–1990 period. If this trend continues, we can expect a further decline in mean forest carbon change during the 2010–2020 decade. Regarding secondary forest growth, we considered forest age and the location in the Amazon, based on the regions identified by Heinrich et al. (2021). Considering the great extent of secondary forests, it is crucial to map the dynamics of this LUCC class.

In estimations of bottom-up emissions, the main emission classes are deforestation, forest degradation, and secondary forest loss. These classes have contributed to the Amazon region becoming a carbon source since 2015. It is crucial to include these LUCC classes in estimates of emissions. Forest degradation, despite not being considered in NCs (or SEEG), is the largest emission source during dry years (i.e., 2010, 2015, and 2016). Dry years (mainly 2015 and 2016) have high emissions in the estimates of bottom-up and top-down fluxes. Furthermore, removals of primary forests, except those in protected areas, are also not included in the NCs and SEEG despite being a large carbon sink, having absorbed −5,901 $TgCO_2$ in the Brazilian Amazon from 2010 to 2018.

Although the bottom-up and the top-down approaches are not completely comparable, this study reveals interesting insights when comparing both approaches. The bottom-up carbon fluxes depend on LUCC input data (activity data) and the emission/removal factors designation; we assumed constant emission factors without including climate variability. The difference in CO_2 flux estimates, according to the LUCC data, is clear when comparing the

SEEG and NC estimates (Wiltshire et al., 2022). On the other hand, top-down estimates capture the forest response to climatic conditions during drier or wetter years, as well as the seasonality of atmospheric fluxes. The top-down atmospheric measurements implicitly include sectors of more emissions and removals (e.g., agriculture, industry) than the LULUCF sector fluxes considered in this study. This may explain why the total top-down estimates are higher than the net bottom-up estimates. To better assess the bottom-up net fluxes, it would be pertinent to include specific fire emissions and consider additional sectors such as agriculture. The continuity of the Amazonian atmospheric measurements is essential to understand the carbon balance in the Amazon, as the deforestation and forest degradation processes have been increasing sharply in recent years. Analyzing both bottom-up and top-down approaches will be necessary to reach the climate targets set by the Paris Agreement (Wiltshire et al., 2022).

5. Conclusion

Land use and cover change dynamics are crucial to understand CO_2 emissions and removals in the Brazilian Amazon. Our bottom-up analyses conducted from 2010 to 2018 reveal that forest is the predominant land cover class, capturing 79% (−5,901 $TgCO_2$) of the total CO_2 removals. Secondary forest is an important carbon sink, capturing 17% of the CO_2 total removals. Throughout the study period, forest cover decreased by 97,066 ha, primarily driven by deforestation and degradation, resulting in emissions of 7,023 $TgCO_2$. Forest carbon stocks are higher in RBA, TAB, and TEF influence regions. SAN and ALF influence regions feature smaller areas of high carbon stocks, with most areas containing patches of forests with lower carbon density.

In the bottom-up estimates, from 2010 to 2014, the net CO_2 flux in the Brazilian Amazon, TAB_TEF, and RBA influence regions indicates a carbon sink. Since 2015, an increase in deforestation and forest degradation has transformed these influence regions into carbon sources, with the highest emission observed in 2016. Regarding SAN and ALF influence regions, the net CO_2 flux shows a sink in 2 years (2011 and 2012), while for the remaining years, it represents a carbon source.

The comparison between the total CO_2 top-down and net bottom-up fluxes reveals that top-down estimates are considerably higher than the bottom-up in the Brazilian Amazon and all influence regions, except for 2017 and 2018. The absolute mean difference between the top-down and the bottom-up is larger in the Brazilian Amazon than in the separate influence regions. Additionally, the bottom-up net CO_2 exhibits less interannual variation compared to the total top-down fluxes.

Regarding CO_2 bottom-up estimates, future methods should focus on evaluating the sensitivity of utilizing multiple datasets, whether derived from remote sensing or *in situ* data, and assess their impacts on the results. The evolution of remote sensing-derived LUCC information is promising, but additional field validation sites are required to enhance and calibrate these datasets. Top-down atmospheric measurements are essential to understand the Amazon forest's CO_2 emissions and removals, and it is important to expand data collection sites in primary forest regions with high carbon density. By considering these aspects, a more

robust comparison between bottom-up and top-down approaches may be achieved.

Among other findings, this study shows the relevance of including forest degradation emissions and carbon uptake from primary forests in the national communications on GHG to the UNFCCC to better reflect the efforts needed to accomplish the Nationally Determined Contribution (NDC) under the Paris Agreement.

Data availability statement

The original contributions presented in the study are included in the article/Supplementary material, further inquiries can be directed to the corresponding author.

Author contributions

GT designed the study, collected, analyzed, and reviewed the data and wrote the manuscript. LG, LB, HC, CS-J, GM, and CV participated in the study design, conceptualization, and refinement. LG, LB, MG, JM, AI, HC, GM, and CS-J provided a thorough review and comments on the manuscript. LG, MG, and JM conceived the basinwide atmospheric measurement program and approach. LD, EA, AI, LB, HC, GT, LM, and LG contributed to the region of influence analysis. CS-J processed the secondary forest and deforestation data. LM, LD, CLC, SC, RN, and CC participated in the GHG concentration analysis. All authors read and approved the final manuscript.

Funding

Acknowledgments

Conflict of interest

The authors declare that the research was conducted in the absence of any commercial or financial relationships that could be construed as a potential conflict of interest.

Publisher's note

All claims expressed in this article are solely those of the authors and do not necessarily represent those of their affiliated organizations, or those of the publisher, the editors and the reviewers. Any product that may be evaluated in this article, or claim that may be made by its manufacturer, is not guaranteed or endorsed by the publisher.

Supplementary material

The Supplementary Material for this article can be found online at: https://www.frontiersin.org/articles/10.3389/ffgc.2023.1107580/full#supplementary-material

References

Aguiar, A. P. D., Ometto, J. P., Nobre, C., Lapola, D. M., Almeida, C., Vieira, I. C., et al. (2012). Modeling the spatial and temporal heterogeneity of deforestation-driven carbon emissions: the INPE-EM framework applied to the Brazilian Amazon. *Glob. Chang. Biol.* 18, 3346–3366. doi: 10.1111/j.1365-2486.2012.02782.x

Albuquerque, I., Alencar, A., Angelo, C., Azevedo, T., Barcellos, F., Coluna, I., et al. (2020). *SEEG 8 Análise das Emissões Brasileiras de Gases de Efeito Estufa e Suas Implicações Para as Metas de Clima do Brasil 1990-2019*. Available online at: https://seeg-br.s3.amazonaws.com/Documentos~Analiticos/SEEG_8/SEEG8_DOC_ANALITICO_SINTESE_1990-2019.pdf

Alencar, A., Zimbres, B., Shimbo, J., Brandão Jr,., A., Arruda, V., et al. (2020). *Nota Metodológica SEEG 8 Setor Mudança de Uso da Terra e Florestas (Versão 1)*. Available online at: https://seeg-br.s3.amazonaws.com/2019-v7.0/notas-metodologicas/SEEG8_NOTA_METODOLOGICA_MUT_2020.11.03.pdf

Almeida, C. A., De Coutinho, A. C., César, J., Mora, D., Adami, M., Venturieri, A., et al. (2016). High spatial resolution land use and land cover mapping of the Brazilian Legal Amazon in 2008 using Landsat-5 / TM and MODIS data. *ACTA Amaz.* 46, 291–302. doi: 10.1590/1809-4392201505504

Aragão, L. E. O. C., Poulter, B., Barlow, J. B., Anderson, L. O., Malhi, Y., Saatchi, S., et al. (2014). Environmental change and the carbon balance of Amazonian forests. *Biol. Rev.* 89, 913–931. doi: 10.1111/brv.12088

Assis, T. O., de Aguiar, A. P. D., von Randow, C., Melo de Paula Gomes, D., Kury, J. N., Ometto, J., et al. (2020). CO₂ emissions from forest degradation in Brazilian Amazonia. *Environ. Res. Lett.* 15:104035. doi: 10.1088/1748-9326/ab9cfc

Baccini, A., Goetz, S. J., Walker, W. S., Laporte, N. T., Sun, M., Sulla-Menashe, D., et al. (2012). Estimated carbon dioxide emissions from tropical deforestation improved by carbon-density maps. *Nat. Clim. Change* 2, 182–185. doi: 10.1038/nclimate1354

Basso, L. S., Gatti, L. V., Gloor, M., Miller, J. B., Domingues, L. G., Correia, C. S. C., et al. (2016). Seasonality and interannual variability of CH₄ fluxes from the eastern Amazon Basin inferred from atmospheric mole fraction profiles. *J. Geophys. Res. Atmos.* 121, 168–184. doi: 10.1002/2015JD023874

Basso, L. S., Marani, L., Gatti, L. V., Miller, J. B., Gloor, M., Melack, J., et al. (2021). Amazon methane budget derived from multi-year airborne observations highlights regional variations in emissions. *Commun. Earth Environ.* 2:246. doi: 10.1038/s43247-021-00314-4

Bullock, E. L., Woodcock, C. E., Souza, C., and Olofsson, P. (2020). Satellite-based estimates reveal widespread forest degradation in the Amazon. *Glob. Chang. Biol.* 26, 2956–2969. doi: 10.1111/gcb.15029

Carreiras, J. M. B., Quegan, S., Le Toan, T., Ho Tong Minh, D., Saatchi, S. S., Carvalhais, N., et al. (2017). Coverage of high biomass forests by the ESA BIOMASS mission under defense restrictions. *Remote Sens. Environ.* 196, 154–162. doi: 10.1016/j.rse.2017.05.003

Cassol, H. L. G., Domingues, L. G., Sanchez, A. H., Basso, L. S., Marani, L., Tejada, G. P., et al. (2020). Determination of region of influence obtained by aircraft vertical profiles using the density of trajectories from the hysplit model. *Atmosphere* 11:1073. doi: 10.3390/atmos11101073

Costa, O. B., da Matricardi, E. A. T., Pedlowski, M. A., Miguel, E. P., and Gaspar, R. (2019). Selective Logging Detection in the Brazilian Amazon. *Floresta Ambient* 26, 1–10. doi: 10.1590/2179-8087.063417

Dubayah, R., Armston, J., Healey, S. P., Bruening, J. M., Patterson, P. L., Kellner, J. R., et al. (2022). GEDI launches a new era of biomass inference from space. *Environ. Res. Lett.* 17:095001. doi: 10.1088/1748-9326/ac8694

EBA (2016). *EBA – Estimativa de Biomassa na Amazônia. Melhor. Dos Métodos Estim. Biomassa e Model. Estim. Emiss. Por Mudança Uso Da Terra.* Available online at: http://www.ccst.inpe.br/projetos/eba-estimativa-de-biomassa-na-amazonia/ (accessed June 6, 2016).

Feldpausch, T. R., Banin, L., Phillips, O. L., Baker, T. R., Lewis, S. L., Quesada, C. A., et al. (2011). Height-diameter allometry of tropical forest trees. *Biogeosciences* 8, 1081–1106. doi: 10.5194/bg-8-1081-2011

Feldpausch, T. R., Lloyd, J., Lewis, S. L., Brienen, R. J. W., Gloor, M., Monteagudo Mendoza, A., et al. (2012). Tree height integrated into pantropical forest biomass estimates. *Biogeosciences* 9, 3381–3403. doi: 10.5194/bg-9-3381-2012

Gatti, L. V., Basso, L. S., Miller, J. B., Gloor, M., Domingues, L. G., Cassol, H. L. G., et al. (2021). Amazonia as a carbon source linked to deforestation and climate change. *Nature* 595, 388–393. doi: 10.1038/s41586-021-03629-6

Gatti, L. V., Gloor, M., Miller, J. B., Doughty, C. E., Malhi, Y., Domingues, L. G., et al. (2014). Drought sensitivity of Amazonian carbon balance revealed by atmospheric measurements. *Nature* 506, 76–80. doi: 10.1038/nature12957

Grace, J. (2016). "The Amazon carbon balance: an evaluation of methods and results" in *Interactions Between Biosphere, Atmosphere and Human Land Use in the Amazon Basin*, eds L. Nagy, B. R. Forsberg, and P. Artaxo (Berlin, Heidelberg: Springer Berlin Heidelberg), 79–100. doi: 10.1007/978-3-662-49902-3_5

Harris, N. L., Brown, S., Hagen, S. C., Saatchi, S. S., Petrova, S., Salas, W., et al. (2012). Baseline map of carbon emissions from deforestation in tropical regions. *Science* 336, 1573–1576. doi: 10.1126/science.1217962

Heinrich, V. H. A., Dalagnol, R., Cassol, H. L. G., Rosan, T. M., de Almeida, C. T., Silva Junior, C. H. L., et al. (2021). Large carbon sink potential of secondary forests in the Brazilian Amazon to mitigate climate change. *Nat. Commun.* 12, 1–11. doi: 10.1038/s41467-021-22050-1

IBGE (2016). *Mudanças Na Cobertura e Uso da Terra 2000-2010-2012-2014.* Rio de Janeiro: IBGE. Available online at: ftp://geoftp.ibge.gov.br/informacoes_ambientais/cobertura_e_uso_da_terra/mudancas/documentos/mudancas_de_cobertura_e_uso_da_terra_2000_2010_2012_2014.pdf

IBGE (2018). *Monitoramento da Cobertura e Uso da Terra do Brasil 2014-2016.* Rio de Janeiro: IBGE. Available online at: https://www.ibge.gov.br/apps/monitoramento_cobertura_uso_terra/v1/ (accessed April 2, 2019).

INPE (2022). *Amazon Deforestation Monitoring Project (PRODES).* INPE. Available online at: http://terrabrasilis.dpi.inpe.br/downloads/

IPCC (2006). "IPCC guidelines for national greenhouse gas inventories volume - iv agriculture, forestry and other land use," in *2006 IPCC Guidelines for National Greenhouse Gas Inventories*, eds H. S. Eggleston, L. Buendia, and K. Miwa (Hayama: Institute for Global Environmental Strategies (IGES)), 1–83.

MapBiomas (2020). *Projeto MapBiomas – Coleção [4.1] da Série Anual de Mapas de Cobertura e Uso de Solo do Brasil.* Available online at: https://mapbiomas.org/colecoes-mapbiomas-1?cama_set_language=pt-BR (accessed September 14, 2020).

MCTI (2016). *Third National Communication of Brazil to the United Nations Framework Convention on Climate Change – Volume III.* Ministério da Ciência Brasília.

MCTI (2020a). *Fourth National Communication of Brazil to the UNFCCC.* Available online at: https://unfccc.int/documents/267657 (accessed January 15, 2021).

MCTI (2020b). *Relatório de Referência: Setor Uso da Terra, Mudança do Uso da Terra e Florestas. Quarta Comunicação Nacional de Emissões e Remoções Antrópicas de Gases de Efeito Estufa.* Available online at: https://www.gov.br/mcti/pt-br/acompanhe-o-mcti/sirene/publicacoes/relatorios-de-referencia-setorial

Nogueira, E. M., Fearnside, P. M., Nelson, B. W., Barbosa, R. I., and Keizer, E. W. H. (2008). Estimates of forest biomass in the Brazilian Amazon: new allometric equations and adjustments to biomass from wood-volume inventories. *For. Ecol. Manage.* 256, 1853–1867. doi: 10.1016/j.foreco.2008.07.022

Olson, D. M., Dinerstein, E., Wikramanayake, E. D., Burgess, N. D., Powell, G. V. N., Underwood, E. C., et al. (2001). Terrestrial ecoregions of the world: a new map of life on earth. *Bioscience* 51:933. doi: 10.1641/0006-3568(2001)051[0933:TEOTWA]2.0.CO;2

Ometto, J. P., Aguiar, A. P., Assis, T., Soler, L., Valle, P., Tejada, G., et al. (2014). Amazon forest biomass density maps: tackling the uncertainty in carbon emission estimates. *Clim. Change* 124, 545–560. doi: 10.1007/s10584-014-1058-7

Pan, Y., Birdsey, R., Fang, J., Houghton, R., Kauppi, P. E., Kurz, W., et al. (2011). A large and persistent carbon sink in the world's forests. *Science* 333, 988–993. doi: 10.1126/science.1201609

Phillips, O. L., Brienen, R. J. W., Gloor, E., Baker, T. R., Lloyd, J., Lopez-Gonzalez, G., et al. (2017). Carbon uptake by mature Amazon forests has mitigated Amazon nations' carbon emissions. *Carbon Balance Manag.* 12, 1–9. doi: 10.1186/s13021-016-0069-2

Rappaport, D. I., Morton, D. C., Longo, M., Keller, M., Dubayah, R., and Dos-Santos, M. N. (2018). Quantifying long-term changes in carbon stocks and forest structure from Amazon forest degradation. *Environ. Res. Lett.* 13:065013. doi: 10.1088/1748-9326/aac331

Silva Junior, C. H. L., Carvalho, N. S., Pessôa, A. C. M., Reis, J. B. C., Pontes-Lopes, A., Doblas, J., et al. (2021). Amazonian forest degradation must be incorporated into the COP26 agenda. *Nat. Geosci.* 14, 634–635. doi: 10.1038/s41561-021-00823-z

Silva Junior, C. H. L., Heinrich, V. H. A., Freire, A. T. G., Broggio, I. S., Rosan, T. M., Doblas, J., et al. (2020). Benchmark maps of 33 years of secondary forest age for Brazil. *Sci. Data* 7:269. doi: 10.1038/s41597-020-00632-w

Silva, C. H. L., Aragão, L. E. O. C., Anderson, L. O., Fonseca, M. G., Shimabukuro, Y. E., Vancutsem, C., et al. (2020). Persistent collapse of biomass in Amazonian forest edges following deforestation leads to unaccounted carbon losses. *Sci. Adv.* 6:eaaz8360. doi: 10.1126/sciadv.aaz8360

Souza, C. M., Shimbo, J. Z., Rosa, M. R., Parente, L. L., Alencar, A. A., Rudorff, B. F. T., et al. (2020). Reconstructing three decades of land use and land cover changes in Brazilian biomes with landsat archive and earth engine. *Remote Sens.* 12:2735. doi: 10.3390/rs12172735

Stein, A. F., Draxler, R. R., Rolph, G. D., Stunder, B. J. B., Cohen, M. D., Ngan, F., et al. (2015). NOAA's HYSPLIT atmospheric transport and dispersion modeling system. *Bull. Am. Meteorol. Soc.* 96, 2059–2077. doi: 10.1175/BAMS-D-14-00110.1

Tejada, G., Görgens, E. B., Ovando, A., and Ometto, J. P. (2020). Mapping data gaps to estimate biomass across Brazilian Amazon forests. *For. Ecosyst.* 7:25. doi: 10.1186/s40663-020-00228-1

Wiltshire, A. J., Randow, C., Rosan, T. M., Tejada, G., and Castro, A. A. (2022). Understanding the role of land-use emissions in achieving the Brazilian Nationally Determined Contribution to mitigate climate change. *Clim. Resil. Sustain.* 1:e31. doi: 10.1002/cli2.31

Withey, K., Berenguer, E., Palmeira, A. F., Espírito-Santo, F. D. B., Lennox, G. D., Silva, C. V. J., et al. (2018). Quantifying immediate carbon emissions from El Niño-mediated wildfires in humid tropical forests. *Philos. Trans. R. Soc. B Biol. Sci.* 373:20170312. doi: 10.1098/rstb.2017.0312